Available online at www.sciencedirect.com
SCIENCE DIRECT®
ELSEVIER
Palaeogeography, Palaeoclimatology, Palaeoecology 235 (2006) 8–27
PALAEO
www.elsevier.com/locate/palaeo

Phyto- and zooplankton paleofluxes during the deposition of sapropel S1 (eastern Mediterranean): Biogenic carbonate preservation and paleoecological implications

M.S. Principato [a,*], D. Crudeli [b], P. Ziveri [c], C.P. Slomp [d], C. Corselli [a], E. Erba [b], G.J. de Lange [d]

[a] *Dipartimento di Scienze Geologiche e Geotecnologiche, Università degli Studi di Milano Bicocca, Piazza della Scienza 4, 20126 Milano, Italy*
[b] *Dipartimento di Scienze della Terra "Ardito Desio," Università degli Studi di Milano, Via Mangiagalli 34, 20133 Milano, Italy*
[c] *Paleoclimatology and Paleoecology Dept., FALW, Vrije Universiteit Amsterdam, De Boelelaan, 1085, 1081HV, Amsterdam, The Netherlands*
[d] *Department of Earth Sciences–Geochemistry, Utrecht University, Budapestlaan 4, 3584 CD, Utrecht, The Netherlands*

Accepted 12 September 2005

Abstract

The relative and absolute abundances and accumulation rates of foraminifera and calcareous nannofossils were quantified in a box core containing sapropel S1 from the Florence Rise area (SE of Cyprus; 2302 m water depth). The main objective of this study was to reconstruct in detail variations in paleoecological conditions of water masses during the deposition of this sapropel. In particular, we qualitatively evaluated the importance of carbonate dissolution on planktonic assemblages to better interpret the abundance profiles obtained from the two investigated taxa.

Selective carbonate corrosion in the core is shown by (1) the decrease in shell mass weight of selected species of planktonic foraminifera, (2) the decrease in accumulation rate of dissolution-susceptible holococcoliths and coccolith species, and (3) the absence of pteropods. However, the presence of other relatively dissolution-susceptible coccolith species throughout all of the S1 interval suggests moderate dissolution.

Florisphaera profunda shows a marked increase in paleofluxes within the sapropel coupled with a decrease in the accumulation rate of the upper–middle photic zone coccoliths, suggesting an ecological depth-separation of the water column, probably characterised by higher nutrient availability at depth and nutrient-depleted surface waters between ~10 and 6.5 kyr BP. In the same interval *Turborotalita quinqueloba* and *Globigerina bulloides*, two foraminiferal species frequently occurring during periods of high fertility, increase in relative abundance. The maximum increase in relative abundance of *Globigerinoides ruber* (var. *alba* and *rosea*) marks the climatic optimum phase and the maximum stratification in surface water that occurred at the beginning of sapropel S1 deposition when the bottom waters were anoxic. An important change in foraminiferal assemblages occurs at ~8 kyr BP and corresponds with a negative shift in $CaCO_3$, Ba and C_{org} contents. This short interval marks the establishment of relatively less anoxic conditions in the bottom water, introducing the last phase of sapropel formation.

* Corresponding author. Tel.: +39 02 64484340; fax: +39 02 64484273.
E-mail address: speranza.principato@unimib.it (M.S. Principato).

doi:10.1016/j.palaeo.2005.09.021

After ~6.5 kyr BP, a progressive re-establishment of normal oceanographic conditions occurred before the real end of the sapropel S1. This transition is well recorded by the reoccurrence and major accumulation rate of the mixing indicator foraminiferal species *Globorotalia inflata* and by the gradual decrease in abundance of *F. profunda*.

Keywords: Calcareous nannofossils; Planktonic foraminifera; Biogenic fluxes; Eastern Mediterranean; Holocene; Sapropel S1

1. Introduction

One of the most pronounced paleoclimatic features in Holocene sediments from the eastern Mediterranean Sea is the occurrence of a distinct organic matter-rich interval identified as sapropel S1 (Cita et al., 1977). This level is usually found a few decimetres below the sediment–water interface in normal pelagic–hemipelagic sediments and was formed between 9.0 and 6.3 ^{14}C kyr BP (Rohling et al., 1997) or between 9.0 and 5.3 ^{14}C kyr BP (Thomson et al., 1999).

Nutrient-enhanced productivity seems to be involved in the formation of sapropels of the eastern Mediterranean. According to Meyers and Doose (1999), the range in degree of organic matter preservation, from good to moderate, suggests that a strong productivity can contribute to improving organic matter preservation on the seafloor. Precessional climate changes that freshened Mediterranean surface waters have been invoked as a primary cause of sapropel formation in the literature (Rossignol-Strick, 1985; Fontugne and Calvert, 1992; Sancetta, 1994). The premise is that increased seasonality in the past, led to intensive precipitation and stronger winds in the Mediterranean area. These cyclic paleoclimatic changes contributed to decreased vertical circulation combined with increased paleoproductivity so that the delivery of marine organic matter to the sea floor was sufficiently large to exhaust the available dissolved oxygen at the bottom. As a consequence, anoxic conditions occurred at the seafloor favouring the preservation of organic matter in bottom sediment. According to this hypothesis sapropel layers reflect high productivity conditions (Meyers and Doose, 1999). In particular, Calvert (1983) suggests that anoxic conditions alone could not have been responsible for accumulation of organic carbon into the sapropels and that a consistent increase in primary productivity has to be invoked. According to Howell and Thunell (1992), during S1 formation the primary productivity changed from 30 g C m^{-2} year^{-1}to 393 g C m^{-2} year^{-1}, which is a value for modern upwelling systems. De Lange and ten Haven (1983) have similarly concluded that organic production significantly increased in the eastern Mediterranean during sapropel S1 deposition.

An oxidation front is currently located at the top of the visual S1, concealing the real thickness of sapropel. At this front, organic carbon and pyrite are oxidized by oxidants diffusing downward from the bottom waters into the sediments. As a result of this oxidation, the organic-rich layer becomes progressively thinner, and iron and manganese oxides precipitate directly above the sapropel (e.g., Ten Haven et al., 1987; De Lange et al., 1989; Van Santvoort et al., 1996; Passier and Dekkers, 2002). This kind of diagenesis produces the so-called "double-manganese-peak" used to define the real top of sapropel (Thomson et al., 1999). Barium is considered a paleoproductivity proxy because of an observed correlation between fluxes of C_{org} and Ba intercepted by sediments traps (Thomson et al., 1999). Therefore, Ba concentrations represent another useful indicator of the original sapropel thickness (Thomson et al., 1995; Van Santvoort et al., 1996).

Several studies have been performed on the composition of planktonic assemblages during the S1 interval. An early study of different microfossil groups (calcareous nannofossils, planktonic foraminifera and pteropods) from the Pleistocene–Holocene sedimentary record of the eastern Mediterranean was performed by Violanti et al. (1991). In this work a paleoenvironmental reconstruction of different sapropel intervals was achieved by the integration of various abundance data of the studied planktonic taxa. After the definition of a more or less detailed planktonic foraminiferal ecozonal scheme for the last 20 kyr in the central Mediterranean sea (Jorissen et al., 1993; Capotondi et al., 1999; Sbaffi et al., 2001), the study of Principato (2003) allowed a partial identification of the assemblage zones (or "ecozones") in the Ionian sea and Levantine basin (eastern Mediterranean). Principato et al. (2003) and Giunta et al. (2003) studied the changes in abundance of planktonic foraminifera and calcareous nannofossils and reconstructed paleoecology and paleoceanography of the S1 interval.

Insight into foraminiferal paleoproductivity variations can be obtained from the estimates of the absolute abundances of these organisms in the sediment, expressed as the number of specimens per gram of

dry sediment (Giunta et al., 2003; Schmiedl et al., 2003; Negri et al., 2003), combined with sediment accumulation rates. This method, for example, allowed evaluation of the role of global and local climate changes on surface circulation in the Benguela region (Giraudeau et al., 2001). Distribution patterns of living planktonic foraminifera can be obtained through plankton tows. Pujol and Vergnaud Grazzini (1995) used this approach to trace the distribution patterns of living planktonic foraminifera, as related to regional hydrography and productive systems in the whole Mediterranean basin. The abundance data for each species were expressed as number of specimens/1000 m^3 water.

Calcareous nannofossils that in the Holocene include coccoliths and a few nannoliths are fossil remains of one of the most important primary producers in the modern Mediterranean and constitute a large part of the biogenic carbonate fraction of sediments (Ziveri et al., 2000; Rutten et al., 2000). Being primary producers and sediment forming, calcareous nannofossils are of great significance in paleoecological–paleoenvironmental reconstructions. The composition of assemblages in the Holocene has been quantified in terms of relative abundance (Violanti et al., 1991; Castradori, 1992, 1993; Crudeli and Young, 2003; Crudeli et al., 2004) and as the number of calcareous nannofossils mm^{-2} (Negri et al., 1999; Negri and Giunta, 2001; Giunta et al., 2003; Principato et al., 2003). These studies provided significant information on environmental variations during the deposition of sapropel S1. However, only few studies have estimated the paleofluxes of nannoflora which are of invaluable significance for improving the interpretation of the fossil record (Ziveri et al., 1999; Ziveri et al., 2001).

The aim of this study is the reconstruction of paleofluxes of different microfossils throughout the last 10 kyr. These data will improve the paleoecological reconstruction of the sapropel S1 interval and will result in a better understanding of the role of organic productivity versus anoxia in sapropel formation, which has given rise to intensive debate in the past decades (Cramp and O'Sullivan, 1999; De Lange et al., 1999).

1.1. Carbonate diagenesis

The original composition of a calcareous biogenic assemblage can be variably altered by carbonate dissolution in the water column and in the sediments. This may lead to misinterpretation of the fossil records. Nevertheless, carbonate dissolution is one of the more difficult processes to quantify in micropaleontological studies.

Biogenic carbonates are commonly very well-preserved in the present Mediterranean bottom sediments because of the moderate depths and the chemical and physical characteristics of this basin. The delicate aragonitic pteropods are very common (Herman, 1981).

In the eastern Mediterranean, carbonate precipitation affects the common calcareous nannofossil species *E. huxleyi*, particularly above and below S1 (Crudeli et al., 2004). The process may be related to diagenetic formation of high-Mg calcite in these sediments (Calvert and Fontugne, 2001; Thomson et al., 2004).

The sapropel carbonate–environment appears complex. Thomson et al. (2004) documented abundant aragonite in S1 and discussed alternative causes for the presence and formation of this carbonate phase, preferring a relation with sulfide formation within the organic matter-rich environment of the sapropel. Dissolution-susceptible species, commonly associated with *F. profunda* in the lower photic zone, decrease in the sapropel of cores from the deep basin. However, it is not clear if this abundance trend is driven by dissolution or if it reflects a primary variation (Thomson et al., 2004).

Quantification of calcareous nannofossil paleofluxes is particularly significant because data can be directly compared with present surface sediment accumulation rates (mainly controlled by export production) and can give an indication of past export production and partial carbonate dissolution.

In addition, in order to qualitatively estimate possible dissolution processes inside and outside the sapropel, we performed a study on foraminiferal weight variations. This approach is compatible with previous studies using foraminiferal shell weights to evaluate the biogenic carbonate preservation in oceanic environment (Broecker and Clark, 2001, 2002; Broecker et al., 2001).

2. Materials and methods

Box core SL9 (Fig. 1) was recovered in the Florence Rise area (south of Cyprus) (34°17.17′N–31°31.36′E) at 2302 m water depth during the R/V Logachev-Cruise 1999. The box core (45.2 cm in length) includes both the visible S1 sapropel (very dark grey to olive grey in colour) and its oxidized part (dark brown in colour). The interval of elevated Ba concentration is used here to indicate the original thickness of S1, whereas the C_{org} content marks the present thickness of the sapropel after post-depositional oxidation processes (Van Santvoort et al., 1996; Thomson et al., 1999). In the following, the term S1 interval or S1 time is used to indicate both the

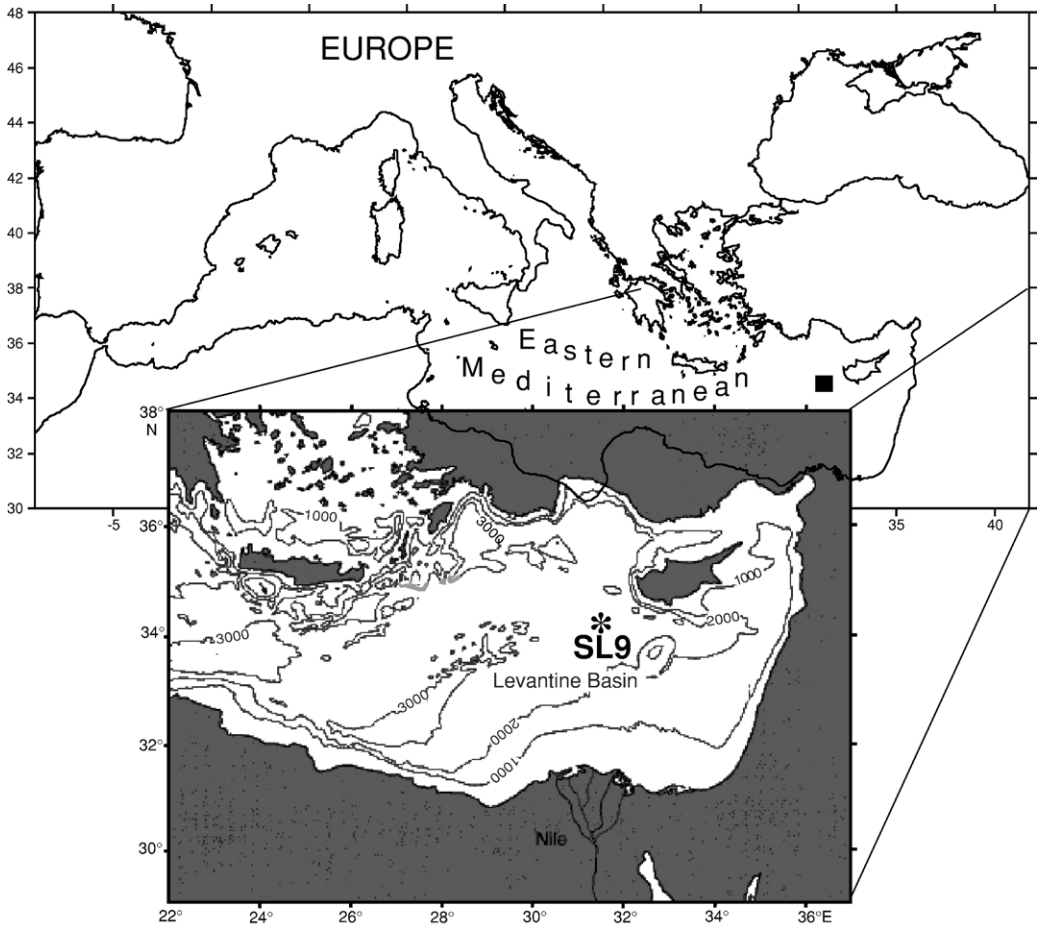

Fig. 1. Map of the eastern Mediterranean Sea indicating the location of the SL9 box core location.

visible and the oxidized S1 according to De Lange et al. (1989), whereas S1 and oxidized S1 indicate the visible S1 and the oxidized S1, respectively.

2.1. Planktonic foraminifera

A total of 44 samples were studied at 1 cm resolution. Each sample was dried at 40 °C and carefully washed through a 63 μm mesh sieve to retain most of the foraminiferal assemblage. The obtained fraction was split into aliquots of at least 300–400 planktonic foraminiferal specimens that were identified and counted, largely following the taxonomic concept of Hemleben et al. (1989). All morphotypes of *G. ruber* are plotted together, distinguishing only the *alba* and *rosea* varieties. The species *Globigerinoides sacculifer* also includes *Globigerinoides trilobus*, using the taxonomic concept of Hemleben et al. (1989), and the 2 species *Globoturborotalita rubescens* and *Globoturborotalita tenella* are included in the same group because of their similar ecological responses. The species *Globigerinita glutinata* includes the morphotypes with and without bulla.

The identified species were quantified as percentages (%) of the total number of planktonic and benthic foraminifera (relative abundance) and as the number of specimens per gram of dry sediment (nr/g) (absolute abundance, AA). Planktonic and benthic foraminiferal accumulation rates (pfAR and bfAR) (number of specimens cm^{-2} kyr^{-1}) were calculated by planktonic foraminiferal abundance data (Ivanova, 1999; Giraudeau et al., 2001):

$$\mathrm{pfAR(bfAR)} = \mathrm{AA} \times \mathrm{SR} \times \mathrm{DBD} \quad (1)$$

where SR is the sedimentation rate in centimetres per thousand years and DBD is the dry bulk density in grams per cubic centimetre. Similarly, the abundance

data of total pteropods were transformed to accumulation rates (pAR).

A preliminary study of foraminiferal weight variations was performed using existing methods (Broecker et al., 2001; Broecker and Clark, 2001, 2002). We selected 3 planktonic foraminiferal species: *G. ruber*, *Orbulina universa* and *G. inflata* after a further fractionation over 250 μm and 355 μm sieves. The picking of these species was carried out on the 250–355 μm fraction. The same number of specimens for each species (60 specimens of *G. ruber*, 20 individuals of *O. universa* and 30 individuals of *G. inflata*) was selected from samples at 2 cm resolution along the core and weighed. Shells without visible secondary calcite growths and with similar size were principally selected to obtain a realistic weight-trend for each species. The choice of two spined and globular species, *G. ruber* and *O. universa* and of a smooth, flat and thick-walled species, *G. inflata*, allowed us to test whether the shell-weight decrease recorded during the S1 interval was dependent on morphological characteristics.

A planktonic foraminiferal "ecozonal" scheme (Capotondi et al., 1999) for core SL9 was obtained following criteria of Principato (2003). Four assemblage zones were recognised from the bottom to the top: PF4a, PF3a, PF2 and PF1a. The meaning of the "PF" code is "planktonic foraminifera," whereas "a" indicates regional characteristics, common to cores from the Levantine Basin. This scheme is based on a micropaleontological study of Principato (2003) and Principato et al. (2003) on the >150 μm fraction of several other cores from the same basin.

2.2. Calcareous nannofossils

2.2.1. Relative abundance

The relative abundance of calcareous nannofossils was estimated in the same 44 samples analysed for the foraminiferal study. Analyses were performed by cross-polarised light microscopy (LM) (Wild Leitz GMBH microscope) at 1250× magnification by counting three to four hundred specimens distributed on smear slides prepared using standard techniques. The relative abundance of minor species was calculated by an additional count of one hundred to one hundred-fifty specimens with the exclusion of *Emiliania huxleyi*, *Gephyrocapsa* and lower photic-zone species (LPZ). These last forms were quantified against one hundred upper–middle photic zone (UPZ-MPZ) species. Counting methods follow the concepts of Matsuoka and Okada (1989) and Castradori (1992, 1993).

2.2.2. Absolute abundance and accumulation rate

The absolute abundance (number of specimens per gram dry sediment, nr/g) of calcareous nannofossil (cnAA) was estimated for 29 samples already analysed in terms of relative abundance. Analyses were carried out at a stratigraphic resolution of 1 cm within the sapropel and at 2 cm outside it.

Samples were prepared using the method described by Ziveri et al. (1999). In addition, the organic matter was oxidized following the procedure described in Bairbakhish et al. (1999). The solution was then wet sieved through a 32 μm mesh, using buffered demineralised water; it was filtered with a low pressure vacuum pump on a mixed cellulose esters filter (MF-Millipore, 0.45 μm pore size, 47 mm diameter) and successively oven-dried at 40 °C for 4–5 h. A filter segment was mounted on a smear slide with a drop of immersion oil. The absolute abundance of calcareous nannofossils was estimated by LM (1250×) by counting forms present in three fields of view (FOW), whereas that of minor species by counting specimens present in seven FOW.

The number of specimens per gram dry sediment was calculated as:

$$N = (\mathrm{efA} \times N')/(\mathrm{cfA} \times w) \quad (2)$$

where efA=effective filtration area (cm^2), N'=number of counted coccoliths, cfA=counted filtration area (cm^2), w=dry weight of the sediment sample.

Accumulation rates of calcareous nannofossils (cnAR) (number of specimens cm^{-2} kyr^{-1}) were estimated from the dry bulk density (DBD, g cm^{-3}) and average sediment accumulation rate (SR, cm kyr^{-1})

$$\mathrm{cnAR} = N \times \mathrm{DBD} \times \mathrm{SR}. \quad (3)$$

2.2.3. Taxonomic remarks

Small *Helicosphaera* specimens were grouped as small *Helicosphaera* spp. This group likely includes *Helicosphaera pavimentum* and *H. hyalina*. *Algirosphaera* coccoliths are assigned to *A. robusta* (Kleijne, 1992) whereas the diverse holococcolith species present in core SL9 (Crudeli et al., in press) are grouped as holococcolith spp. *Umbilicosphaera sibogae* and *U. foliosa* are grouped as *Umbilicosphaera* spp. *Rhabdosphaera clavigera* and *R. stylifera* are lumped as *Rhabdosphaera* spp. Moderately to highly calcified *Umbellosphaera* and *Syracosphaera* coccoliths (from qualitative observations), not identifiable at species level, were separately counted and are here termed OG (overgrown) *Umbellosphaera* and OG *Syracosphaera*.

2.3. Geochemical analyses

Sediment samples at 0.5 cm depth resolution were freeze-dried and ground in an agate mortar. Total concentrations of Al, Ba and Ca were determined after digestion in a mixture of HF, HNO_3 and $HClO_4$ and final solution in 1 M HCl using ICP-OES (Perkin Elmer Optima 3000). The accuracy of the measurements was monitored by including laboratory standards. The error in the analysis was <5% for all elements. Organic C was determined on a Fisons Instruments CNS NA 1500 analyser. Inorganic C was removed prior to the analysis by shaking the sample with 1 M HCl twice (12 h and 4 h). The sample was then rinsed with demineralised water twice, freeze-dried and ground in an agate mortar. Tests showed that the amount of organic C hydrolysed by the HCl treatment was negligible. The error in the analysis was less than 1%.

Dry bulk densities were calculated from the weight loss upon freeze-drying of sediment samples taken at 0.5 cm resolution, assuming a sediment density of 2.65 g cm^{-3} and a density of seawater of 1.028 g cm^{-3}.

2.4. Age model

A calibration line based on four ^{14}C AMS dating on *G. ruber* from the >150 μm fraction was used to reconstruct a realistic temporal scale. The investigated interval slice is the Holocene, that is the last 10 kyr. According to this chronological scheme the duration of the S1 interval exceeds 4 kyr, considering the black interval and the oxidized level above it. The depth scale in the core was converted to an uncalibrated ^{14}C age scale (kyr BP) on the basis of a calculated average sedimentation rate of 4.6 cm /kyr.

3. Results

3.1. Micropaleontology

3.1.1. Planktonic foraminifera

Relative abundance data of nine selected planktonic foraminiferal species from >63 μm fraction are shown in Fig. 2. Simple diversity for planktonic foraminifera is lower (10 species) in the lower part of S1, whereas it is higher (16–17 species) in the oxidized S1 and just below the base of sapropel (Fig. 3a). The Shannon diversity index changes from values <1 in the lower–middle part of sapropel (0.89 at 9.03 kyr BP) to values >1 in the oxidized S1, in the normal pelagic sediments below (1.67 at 9.95 kyr BP) and above the sapropel (1.50 at 1.55 kyr BP, 1.55 at 0.44 kyr BP) (Fig. 3a).

The relative abundance curves clearly show that the >63 μm fraction is dominated by the presence of *T. quinqueloba*, which reaches a maximum in the abundance curve at the base of sapropel. *G. ruber alba* and *G. ruber rosea* abundance curves show the maximum increase in the lower part of S1, strongly decreasing in the remaining sapropel interval. In particular, the *G. ruber alba* abundance curve increases again after sapropel deposition up to the top of the core, whereas *G. ruber rosea* almost disappears after the S1 interval.

The relative abundance curve of *G. sacculifer*/*trilobus* shows a typical trend (Principato et al., 2003) during S1 time with an increase in abundance at the base of S1, a temporary disappearance into S1 and a new increasing trend in the upper part of sapropel. *O. universa* is present within S1, but it is more abundant after sapropel formation, in the upper part of the core.

G. inflata and *Truncorotalia truncatulinoides* both disappear in the lower part of the sapropel. *G. inflata* temporary reappears with a significant increase in relative abundance in the upper part of S1, whereas *T. truncatulinoides* totally disappears at the bottom of S1. *N. pachyderma* dextral abundance trend is comparable with the *G. inflata* one with the difference that the first species is continuously present almost up to the core top.

The curve of *G. bulloides* shows an increase into the visible S1 and abruptly decreases in the upper part of the sapropel interval.

In Fig. 2 the absolute abundances (nr/g) of the nine selected foraminiferal species are transformed to accumulation rates (nr. specimens cm^{-2} kyr^{-1}). An increasing trend in pfAR values of *G. ruber rosea* characterises all the S1 interval. Species disappearance is detected in the upper part of the oxidized S1. The curve of *G. ruber alba* shows an increase in accumulation rate at the S1 bottom, even if the maximum value is recorded in the oxidized S1. A weak increase in pfAR of *O. universa* characterises almost the entire sapropel interval, but the species increases mostly in the post-S1 interval, with the maximum value of pfAR at the top of the core. The accumulation rates of *G. sacculifer*/*trilobus*, *N. pachyderma* dextral, *G. inflata* and *T. truncatulinoides* strongly decrease and the species disappear about at the same level in the lowest S1; however, only *T. truncatulinoides* totally disappears. The other three species have a significant increase in accumulation rate in the upper S1 or in its oxidized portion, respectively. *G. sacculifer*/*trilobus* and *N. pachyderma* dextral, after an abrupt decrease in accumulation rate at the top of the oxidized S1, continue to be represented in the most recent interval with various

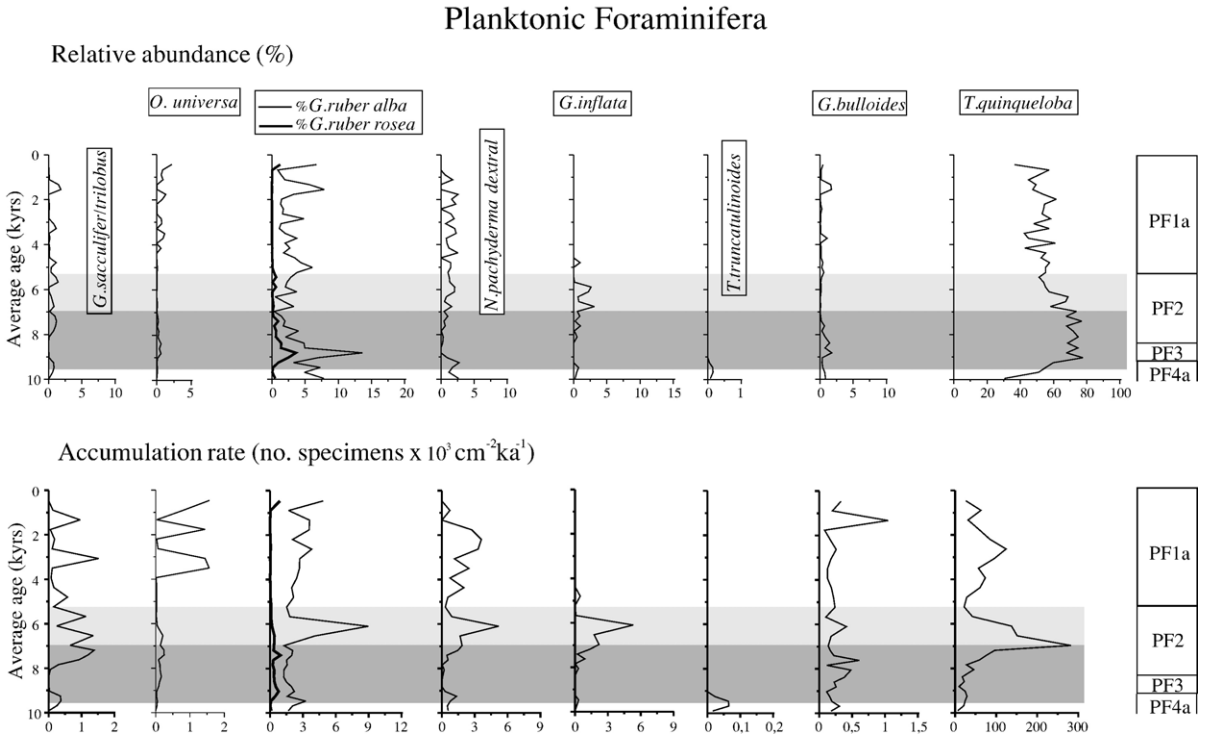

Fig. 2. Relative abundance (%) and accumulation rate (pfAR) of the most representative planktonic foraminiferal species. S1 and oxidized S1 are indicated in dark grey and light grey respectively. On the right side of upper graphs the boundaries of 4 "assemblage zones" (Fp1a–Fp4a), according to Principato (2003), are reported.

oscillations. In contrast, *G. inflata* decreases in accumulation rate and disappears just above the oxidized S1 top.

The occurrence of *G. bulloides* is characterised by various oscillations and a maximum positive peak in the upper part of core. The curve of *T. quinqueloba*, the most represented species in the >63 μm fraction, shows a trend comparable with that of *G. ruber alba*: the accumulation rate of *T. quinqueloba* gradually increases into the S1 and reaches the maximum value in the upper part of sapropel, about in correspondence with the boundary between S1 and the oxidized S1.

The measurements of shell weight outside and into the sapropel interval gave the following results. We obtained almost continuous signals of shell weight variations for the two species *G. ruber* and *O. universa* (Fig. 4). Weight measurements for *G. inflata* were only possible in a portion of the sapropel interval and just below it, where the species is present (Fig. 2). *G. ruber* and *O. universa* show an abrupt decrease in weight at the beginning of S1 deposition, with minimum values of 0.8 μm (Fig. 4). *O. universa* shows the lowest weight (0.6 μm) at the top of the sapropel interval. *G. inflata* has a minimum value (0.5 μm) about in the middle of S1 interval, at the top of the visible sapropel. The trend of this species shows a clear increase in weight values proceeding towards the top of S1 interval with a maximum of 1.8 μm in the last sample containing *G. inflata*.

3.1.2. Calcareous nannofossils

The calcareous nannofossil assemblage includes 44 coccoliths taxa (of which 8 holococcoliths, Crudeli et al., in press) and the two *Incertae Sedis F. profunda* and *Gladiolithus flabellatus* (Jordan and Kleijne, 1994) (Table 1; Figs. 3b and 5). The simple diversity has average values of 26. The minimum (20 species) occurs just below the S1/oxidized S1 limit (7.41 kyr BP), the maximum (31 taxa) close to the top of the core (2.85 kyr). The diversity index does not change consistently throughout the last 10 kyr (Shannon diversity index, 1.0–1.7), showing minimum values just above the S1/oxidized S1 limit (Fig. 3b). The relative abundance and accumulation rates of the most abundant/significant groups are compared in Fig. 5. Table 1 reports relative abundance and accumulation rates of other minor coccoliths.

The dominant *E. huxleyi* (70–80%) has an average accumulation rate of 300×10^8 specimens cm^{-2} kyr^{-1}; accumulation rates of other upper–middle Photic Zone

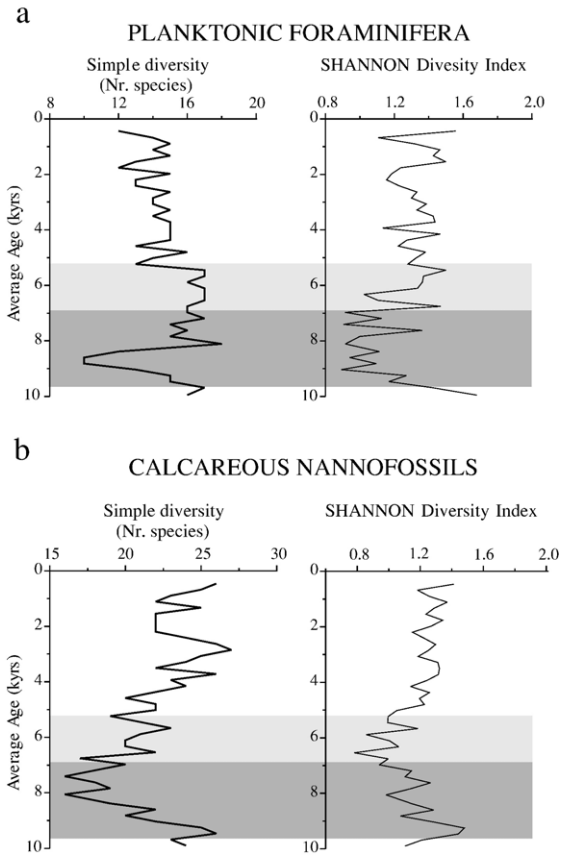

Fig. 3. Simple diversity and Shannon Diversity Index (SDI) of planktonic foraminifera (a) and calcareous nannofossils (b).

(UPZ-MPZ) coccoliths amount to 50×10^8 specimens cm^{-2} kyr^{-1}. Fluxes of *E. huxleyi* decreases below the bottom of S1 and shows a maximum at ~6 kyr BP. *H. carteri* has paleofluxes $>3 \times 10^8$ cm^{-2} kyr^{-1} until about 8 kyr BP and decreases upward where, as small *Helicosphaera* spp., is rare to absent above the sapropel.

The abundance curve of *Syracosphaera pulchra* shows a weak increase within the visual sapropel. By contrast, the species decreases in fluxes within the sapropel and shows a major increase starting at about 6.5 kyr BP. *Rhabdosphaera* spp. display an increase in relative abundance from the base of S1 and decreases upward, whereas the same species has a maximum peak in accumulation rate after the top of S1.

Umbellosphaera tenuis displays two positive peaks (%) within the visual sapropel that are detected in the accumulation rate profile. *Umbilicosphaera* spp. reach maximum values in abundance just below the top of S1. The group increases in accumulation rates in S1 with maximum values just above the top of the sapropel. Paleofluxes of holococcolith spp. abruptly decrease in S1 and, after a temporary disappearance within a short interval of S1, they increase again from just after the S1/oxidized S1 boundary. *Braarudosphaera bigelowii* is mostly confined to the post-sapropel interval. The paleofluxes of *F. profunda* are high from below the S1 bottom and decrease upwards after about 6.5 kyr BP. *A. robusta* and *G. flabellatus* paleofluxes are of moderate magnitude only above the sapropel. Reworked forms (Cretaceous and Neogene) are present along the whole core (5%, average).

Calcareous nannofossil assemblage zones (ecozones) are defined in the Holocene eastern Mediterranean sedimentary interval (Giunta et al., 2003; Principato et al., 2003). In core SL9, we recognised the upper boundaries of ecozones C4 and C3 (Principato et al., 2003) (Fig. 5). We did not find the upper boundary of ecozone C2 (last common occurrence of *B. bigelowii*), so that we located it at the top of the sapropel; the C2 interval is generally characterised by a decrease in *F. profunda* abundance curve and this trend was also recognised in the SL9 core.

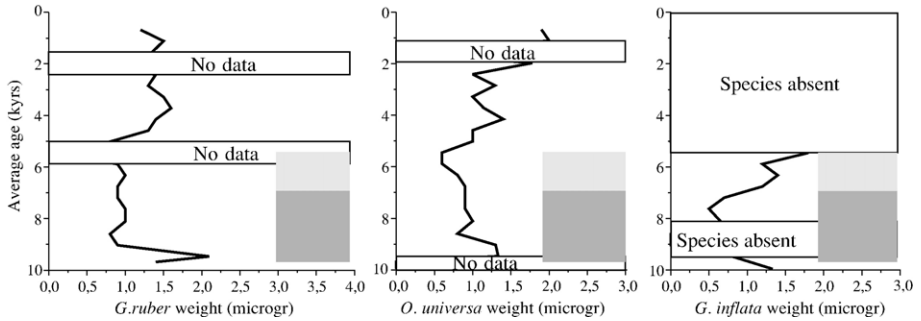

Fig. 4. Shell weights of three selected species of planktonic foraminifera. S1 and oxidized S1 are indicated in dark grey and light grey respectively. Weight measurements are not recorded in two intervals (~1.5–2.5, 5–6 kyr) for *G. ruber* and one interval (~1–2 kyr) for *O. universa*; in these samples the shells selected from the 250–355 μm fraction were not abundant enough for weight estimation.

Table 1
Accumulation rates and relative abundance of minor forms of coccoliths

Centimetre from top	Age (kyr)	*D. tubifera* (%)	*Coronosphaera* spp. (%)	Other *Syracosphaera* spp. (%)	*C. leptoporus* spp. (%)	*C. pelagicus* (%)	*N. coccolithomorpha* (%)	*Oolithotus* spp. (%)	*Pontosphaera* spp. (%)	*Anaplosolenia* spp. (%)	*Ceratolithus* spp. (%)	*H. perplexus* (%)	*S. apsteinii* (%)	Other (%)
0.7	0.5	10.3	1.7	7.3	3.0	0.0	0.9	0.9	0.4	7.7	0.0	0.4	0.4	3.0
1.7	0.7	10.9	2.5	4.6	4.2	0.4	0.0	0.8	0.0	8.4	0.0	0.0	0.0	3.8
2.7	0.9	10.8	1.4	7.2	2.3	0.0	0.0	0.0	0.5	6.8	0.0	0.0	0.0	6.3
3.7	1.1	14.0	2.3	5.4	3.1	0.0	0.8	0.0	0.8	7.0	0.0	0.0	0.8	4.7
4.7	1.3	10.6	1.5	4.0	5.5	0.0	0.0	1.0	0.5	4.5	0.0	0.0	1.0	4.0
5.7	1.5	3.4	2.1	6.8	3.4	0.0	0.7	0.0	0.7	5.5	0.0	0.0	0.7	6.8
6.7	1.8	6.8	1.7	2.8	4.0	0.0	0.0	0.0	0.0	6.3	0.0	0.0	0.0	8.5
7.7	2.0	5.5	3.9	11.0	2.2	0.0	1.1	0.0	0.0	7.2	0.0	0.0	0.0	5.0
8.7	2.2	7.7	2.7	7.7	2.7	0.0	0.0	1.1	0.0	7.7	0.0	0.0	0.0	7.1
9.7	2.4	9.3	4.1	9.3	2.3	0.6	0.0	0.0	0.0	5.8	0.0	0.6	0.0	7.0
10.7	2.6	2.0	4.1	6.8	1.4	0.0	0.7	0.7	0.0	6.8	0.0	0.0	0.0	5.4
11.7	2.8	6.8	3.7	7.9	0.5	0.0	1.0	0.5	0.5	4.2	0.0	0.0	0.0	7.3
12.7	3.1	5.7	3.4	2.9	1.7	0.0	0.0	2.9	0.0	9.7	0.0	0.0	0.0	5.1
13.7	3.3	5.4	3.9	6.9	2.5	0.0	1.0	1.5	0.0	8.8	0.0	0.5	0.0	6.9
14.7	3.5	6.7	3.4	4.5	2.8	0.6	1.7	2.2	0.6	9.5	0.0	0.0	0.0	5.6
15.7	3.7	2.1	2.7	11.8	3.2	0.5	2.1	2.1	0.0	4.3	0.0	0.0	0.5	5.3
16.7	3.9	6.5	2.6	5.8	3.9	0.0	0.6	2.6	0.6	4.5	1.3	0.6	0.6	3.2
17.7	4.2	6.6	3.3	7.0	4.2	0.0	1.4	1.9	0.5	8.9	0.0	0.5	0.5	5.6
18.7	4.4	4.0	1.3	8.0	2.2	0.0	0.4	0.9	0.4	8.9	0.0	0.0	0.0	7.6
19.7	4.6	3.8	3.3	6.6	2.4	0.0	0.9	1.4	0.0	10.9	0.0	0.0	0.5	3.3
20.7	4.8	5.2	3.1	6.2	3.6	0.5	0.5	1.0	1.5	11.3	0.0	0.0	0.0	3.6
21.7	5.0	2.3	1.9	7.9	2.8	0.0	2.8	1.9	0.0	10.2	0.0	0.0	0.5	4.7
22.7	5.2	3.8	4.2	6.8	2.5	0.0	1.3	1.7	0.8	7.2	0.0	0.4	0.0	4.2
23.7	5.5	4.7	3.0	6.4	3.4	0.0	0.8	2.5	0.8	10.2	0.4	0.0	0.4	2.1
24.7	5.7	3.1	4.6	9.2	2.3	0.8	0.8	0.8	0.0	11.2	0.0	0.0	0.0	3.5
25.7	5.9	5.3	5.3	14.6	4.1	0.6	0.6	1.2	0.6	9.4	0.6	0.0	0.0	1.8
26.7	6.1	4.7	3.2	11.1	4.2	0.0	0.0	0.0	0.0	9.5	0.0	0.0	0.0	1.1
27.7	6.3	4.6	2.8	9.2	2.8	0.5	0.5	0.0	0.9	8.3	0.5	0.0	0.0	1.4
28.7	6.5	3.1	3.5	8.3	2.2	0.4	0.0	0.0	1.3	7.0	0.0	0.4	0.4	2.6
29.7	6.8	6.4	2.9	9.8	2.3	1.2	0.6	0.0	0.6	13.3	0.0	0.6	0.6	0.0
30.7	7.0	5.2	4.0	14.5	3.5	0.0	0.0	0.0	0.0	6.4	0.6	0.0	0.6	0.0
31.7	7.2	5.1	4.1	10.8	2.1	0.5	0.0	0.0	1.5	5.6	0.0	0.0	0.5	0.0
32.7	7.4	2.4	5.3	14.2	1.8	0.6	0.0	0.0	0.0	6.5	0.6	0.0	1.2	0.0
33.7	7.6	6.2	2.9	16.3	1.4	0.5	0.5	0.0	0.5	5.3	0.5	0.0	0.0	0.5
34.7	7.8	4.2	3.2	13.2	4.2	0.0	0.0	0.0	1.6	8.4	0.5	0.0	0.0	0.0
35.7	8.1	4.8	3.8	8.1	2.7	0.0	0.0	0.0	0.0	8.6	0.0	0.0	0.5	0.0

37.2	8.4	4.4	3.9	10.3	4.4	0.5	0.5	0.0	0.5	8.3	0.5	0.0	0.0	0.5
38.2	8.6	7.2	2.9	5.8	3.4	0.5	0.0	0.0	1.0	6.3	0.0	0.0	0.5	1.0
39.2	8.8	2.5	2.5	10.3	3.9	0.0	1.0	0.0	1.5	4.9	0.0	0.0	1.0	0.0
40.2	9.0	3.4	2.9	9.6	0.5	0.0	0.0	0.0	3.4	4.8	0.0	0.0	1.4	1.9
41.2	9.3	4.7	2.4	9.9	0.9	0.0	0.0	0.5	0.9	2.4	0.5	0.0	0.0	4.2
42.2	9.5	4.4	1.9	12.0	1.3	0.6	0.0	0.0	0.6	5.1	0.0	0.0	0.6	3.8
43.2	9.7	4.6	0.0	9.2	1.7	1.2	1.2	0.0	0.6	2.9	0.0	0.0	1.7	5.8
44.2	9.9	3.3	1.9	8.5	1.4	0.0	0.5	0.0	0.0	7.0	0.0	0.0	0.5	5.2

Centimetre from top	Age (kyr)	*D. tubifera* (nr. × 108/ cm^2/kyr)	*Coronosphaera* spp. (nr. × 108/ cm^2/kyr)	Other *Syracosphaera* spp. (nr. × 108/ cm^2/kyr)	*C. leptoporus* spp. (nr. × 108/ cm^2/kyr)	*C. pelagicus* (nr. × 108/ cm^2/kyr)	*N. coccolithomorpha* (nr. × 108/cm^2/kyr)	*Oolithotus* spp. (nr. × 108/ cm^2/kyr)	*Pontosphaera* spp. (nr. × 108/ cm^2/kyr)	*Anaplosolenia* spp. (nr. × 108/ cm^2/kyr)	*Ceratolithus* spp. (nr. × 108/ cm^2/kyr)	*H. perplexus* (nr. × 108/ cm^2/kyr)	*S. apsteinii* (nr. × 108/ cm^2/kyr)	Other (nr. × 108/ cm^2/kyr)
0.7	0.5	2.3	1.4	3.3	1.8	0.0	0.4	0.6	0.0	3.5	0.0	0.2	0.2	0.0
2.7	0.9	0.0	1.9	2.1	2.3	0.0	0.2	0.5	0.0	3.0	0.0	0.0	0.5	0.0
4.7	1.3	2.1	1.4	2.1	1.4	0.0	0.0	0.7	0.5	3.3	0.0	0.0	0.0	0.0
6.7	1.8	2.4	0.7	3.1	1.4	0.2	0.0	0.5	0.0	3.4	0.0	0.2	0.0	0.2
8.7	2.2	1.8	1.1	4.1	1.1	0.0	0.2	0.0	0.7	3.4	0.0	0.2	0.0	0.5
10.7	2.6	1.4	1.4	2.4	1.4	0.2	0.0	0.5	0.0	2.4	0.0	0.5	0.0	0.2
12.7	3.1	2.1	1.2	2.8	2.4	0.0	0.0	1.2	0.2	2.6	0.0	0.0	0.0	0.2
14.7	3.5	0.6	0.6	3.4	1.3	0.0	0.0	0.8	0.0	2.5	0.2	0.2	0.0	0.0
16.7	3.9	0.5	1.2	3.1	2.4	0.0	0.2	0.7	0.7	4.2	0.0	0.5	0.0	0.2
18.7	4.4	0.9	1.4	4.0	2.3	0.0	0.2	0.9	0.2	2.6	0.0	0.2	0.0	0.0
20.7	4.8	0.4	2.0	3.1	2.0	0.0	0.4	1.3	0.4	4.2	0.0	0.2	0.0	0.0
22.7	5.2	3.0	2.2	3.4	1.2	0.2	0.4	1.4	0.2	3.4	0.0	0.2	0.0	0.4
24.7	5.7	3.7	1.2	4.8	1.5	0.0	0.4	0.2	0.0	5.2	0.0	0.2	0.2	0.2
26.7	6.1	0.6	1.1	5.0	1.5	0.0	0.0	0.0	0.2	2.6	0.4	0.0	0.0	0.0
28.7	6.5	0.7	1.2	2.7	0.8	0.0	0.0	0.0	0.5	1.0	0.0	0.3	0.2	0.0
30.7	7.0	0.5	0.6	2.9	0.3	0.0	0.0	0.0	0.2	1.3	0.3	0.0	0.2	0.0
31.7	7.2	0.5	0.9	2.5	0.3	0.0	0.0	0.0	0.3	0.5	0.2	0.0	0.2	0.0
32.7	7.4	0.0	0.8	3.0	0.6	0.2	0.0	0.0	0.2	0.5	0.0	0.0	0.0	0.0
33.7	7.6	0.0	0.7	3.2	1.2	0.2	0.0	0.0	0.2	1.2	0.0	0.0	0.0	0.0
34.7	7.8	0.2	1.0	2.6	1.0	0.2	0.0	0.0	0.0	1.2	0.2	0.2	0.3	0.0
35.7	8.1	0.0	1.0	2.8	0.7	0.2	0.0	0.0	0.0	1.0	0.2	0.0	0.0	0.0
37.2	8.4	0.3	0.8	1.1	1.1	0.3	0.0	0.0	0.5	0.2	0.0	0.0	0.2	0.0
38.2	8.6	0.2	0.8	2.4	0.3	0.2	0.0	0.0	0.3	0.8	0.2	0.0	0.2	0.0
39.2	8.8	0.2	1.4	3.1	0.8	0.2	0.0	0.2	0.3	1.2	0.2	0.0	0.2	0.2
40.2	9.0	0.3	0.7	2.3	0.7	0.0	0.2	0.0	0.3	0.8	0.3	0.0	0.2	0.0
41.2	9.3	0.5	1.4	4.0	0.5	0.0	0.0	0.0	0.3	2.3	0.0	0.0	0.2	0.0
42.2	9.5	0.4	0.4	4.7	1.0	0.2	0.0	0.6	0.6	1.2	0.0	0.0	0.0	0.0
43.2	9.7	0.8	0.6	4.4	0.6	0.0	0.0	0.0	0.8	2.3	0.2	0.0	0.4	0.0
44.2	9.9	0.5	2.3	4.8	1.1	0.2	0.5	0.0	0.0	2.7	0.0	0.2	0.0	0.0

The S1 and ox. S1 intervals are evidenced by black thin lines.

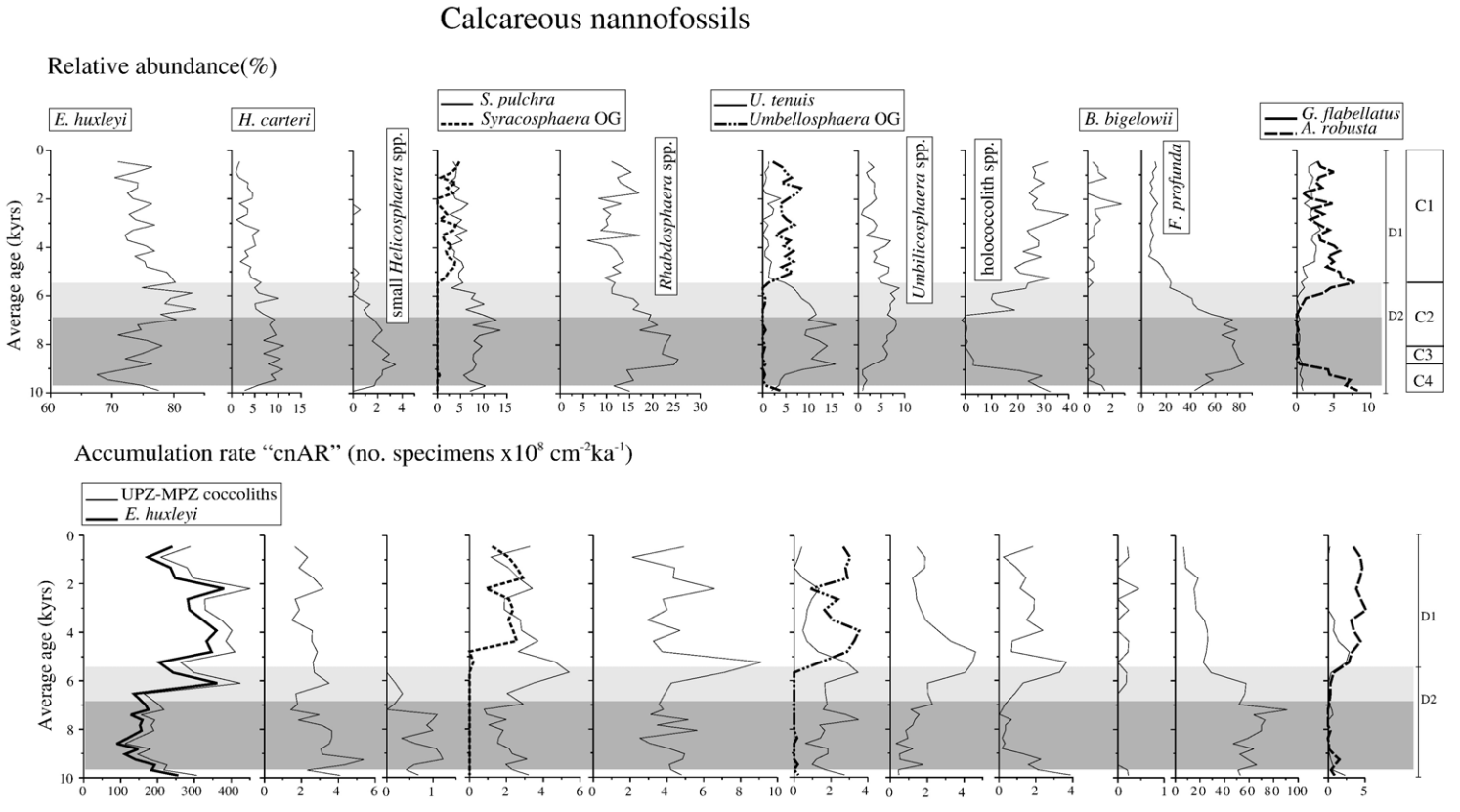

Fig. 5. Comparison between relative abundance (upper line) and accumulation rate (lower line) of calcareous nannofossils. S1 and oxidized S1 are indicated in dark grey and light grey respectively. The depth of the diagenetic intervals recognised in this core (D1 and D2, Crudeli et al., 2004) are shown on the right side of the panel. In the right side (upper line), the subdivision in ecozones for core SL9 obtained applying the definition of Principato et al. (2003) is displayed. See text for further explanation. Upper line, from the left side: *E. huxleyi*, which includes normally preserved and variably overgrowth forms (Crudeli et al., 2004)–*H. carteri*–small *Helicosphaera* spp. (*H. pavimentum* and *H. hylina*)–*S. pulchra* and OG *Syracosphaera*–*Rhabdosphaera* spp.–*U. tenuis* and OG *Umbellosphaera*–*Umbilicosphaera* spp.–holococcolith spp.–*B. bigelowii*–*F. profunda*–*G. flabellatus*. and *A. robusta*. At the left side of the lower line the accumulation rate of *E. huxleyi* and of the UPZ-MPZ forms, including *E. huxleyi*, is shown.

3.2. Geochemical data

$CaCO_3$ concentrations in the sapropel are generally lower than in surrounding layers (Fig. 6a).

The profile of Ba/Al in box core SL9 shows a Gaussian-shape starting at the lower part of S1 and returning to initial values (around 25 ppm/%) at about 5.2 kyr BP (Fig. 6b). A brief drop in Ba/Al (153–159 ppm/%) is visible between 7.8 and 8.0 kyr BP (dotted interval in Fig. 6b), whereas the maximum value (228 ppm/%) is recorded at 7.35 kyr BP.

After an initial increasing trend in concentration, the C_{org} content shows an abrupt negative peak (1.84%) at 7.8 kyr BP, whereas the maximum value (2.64%) is at 7.5 kyr BP. In the remaining part of the box core, C_{org} contents are almost constant and very low (<0.5%) (Fig. 6c).

4. Discussion

4.1. Micropaleontological indications of carbonate dissolution

The annual coccolith accumulation rate in eastern Mediterranean surface sediments changes as a function of the location (100×10^8 to 58.7×10^8 specimens m^{-2} $year^{-1}$, Ziveri et al., 2000; 300×10^8 to 6×10^8 coccoliths cm^{-2} kyr^{-1}, Ziveri et al., 1999). Various processes occurring at the sea floor or within the first centimetres of sediments can alter the composition of calcareous assemblages (Steinmetz, 1994 and reference therein). The average total UPZ-MPZ coccolith accumulation rates from non-sapropel sediments (Fig. 5) are comparable, suggesting absence of significant post-depositional dissolution of the calcareous nannoflora. *E. huxleyi* coccoliths from non-sapropel sediments of eastern Mediterranean are variably affected by carbonate precipitation as suggested by consistent values of the *E. huxleyi*-overgrowth index (EXO) (Crudeli et al., 2004). *U. tenuis* shows a behaviour similar to that of *E. huxleyi* at carbonate diagenesis (Winter, 1982), and indeed OG forms accompanied by a variable amount of OG *Syracosphaera* are common outside S1 (Fig. 5). A possible link between carbonate precipitation on coccoliths and diagenetic formation of high-Mg calcite (Calvert and Fontugne, 2001; Thomson et al., 2004) still needs to be established.

The decrease in number of calcareous nannofossil per square millimetre within S1 sediments suggests a decrease in coccolithophore productivity during sapropel deposition (e.g., Negri and Giunta, 2001). This decrease, expressed as the decrease in accumulation rates of the total nannoflora in S1 from core SL9 (Fig. 7), could be partially due to selective dissolution. Holococcolith spp. are likely dissolved within the sapropel (Crudeli et al., in press). The fact that the curves of more dissolution-susceptible species, *G. flabellatus* and *A. robusta*, show a profile similar to that of holococcoliths spp. (Fig. 5) also suggests effects of dissolution. Similarly, *B. bigelowii* is susceptible to dissolution (Thierstein, 1980), and the decrease in S1 may be due to preservation factors.

The species discussed above are minor components of the assemblage, and they would imply only minor carbonate dissolution. Nonetheless, the dominant *E. huxleyi* is susceptible either to overgrowth or dissolu-

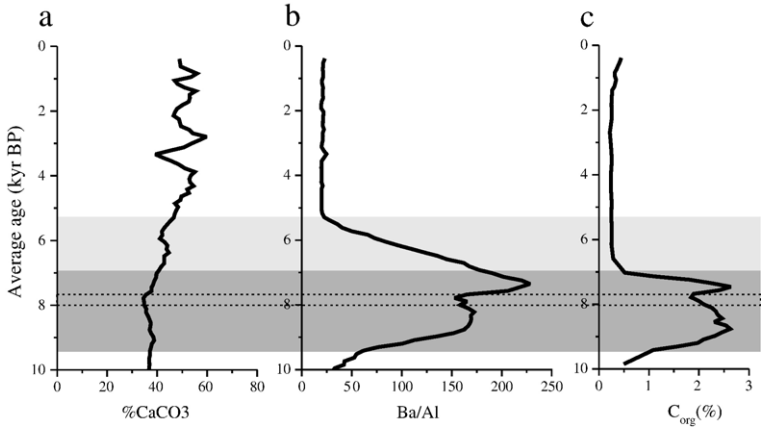

Fig. 6. $CaCO_3$ (%) (a), Ba/Al (ppm/%) (b) and C_{org} (%) (c) versus age (kyr). The S1 and oxidized S1 are indicated as dark grey and light grey areas, respectively. The Ba profile is normalized to Al to correct for fluctuations in carbonate content. The negative peak of Ba/Al and C_{org} recorded within S1 is indicated by a dotted area.

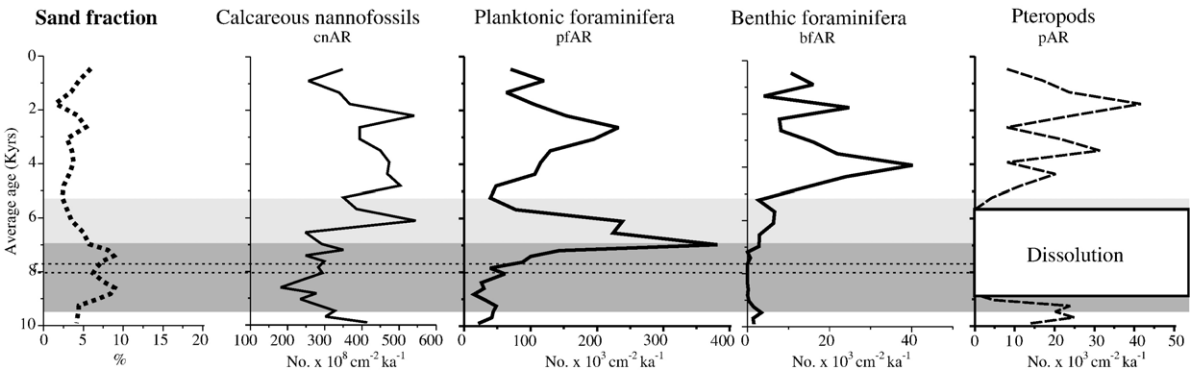

Fig. 7. Sand fraction (%), total paleofluxes of calcareous nannofossils (cnAR), planktonic foraminifera (pfAR) and pteropods (pAR). S1 (dark grey) and oxidized S1 (light grey) are reported on the figure. The negative peak of Ba/Al and C_{org} recorded within S1 is indicated by a dotted area. The white rectangle indicates the interval where pteropods are absent.

tion (Ziveri et al., 1999; Crudeli et al., 2004). Its decrease in S1 (Fig. 5) may result from partial carbonate corrosion. Either way, the sporadic occurrence of holococcoliths (Fig. 5) and the consistent presence of other delicate species (e.g., *Discosphaera tubifera*, *Umbilicosphaera* spp.) (Roth and Berger, 1975; Roth and Coulbourn, 1982) within the sapropel of core SL9 suggest that carbonate dissolution was probably weak.

The curve of the pteropods shows an increase in sedimentation rate at the bottom of the sapropel; these organisms disappear in most of S1 and increase again in the upper part of core where they reach maximum pAR values (Fig. 7). Since aragonite is one of the more soluble carbonate phases (Berner and Honjo, 1981), the pattern within the S1 interval of core SL9 (Fig. 7) and other sites from the region (Giunta et al., 2003) may be due to dissolution rather than to primary variation. Planktonic foraminifera show an abrupt increase in sedimentation rate in the upper part of sapropel. The general increase in the sand content (Fig. 7) of the visible S1 sediments can be attributed to the abundance of various mineral components such as gypsum crystals and pyrite aggregates that characterise the total sand fraction together with foraminiferal shells.

A decrease in weight is detected at the beginning of the S1 period for the three foraminiferal species *G. ruber*, *O. universa* and *G. inflata* (Fig. 4). The interval where these species decrease in weight roughly corresponds to the interval where selected holococcoliths, other delicate forms (*G. flabellatus* and *A. robusta*) and pteropods are rare to absent.

Generally, foraminiferal shells from the sapropel interval are slightly lighter than shells above and below S1. For *G. ruber*, this could be partially related to the dominance of the morphotype *G. ruber* s.s. in S1 with respect to the other more compact morphotypes (*Globigerinoides gomitulus*, *Globigerinoides elongatus* and morphotypes intermediate between them) listed under *G.* ex gr. *ruber* according to Capotondi et al. (1999). The fact that, within S1, a decrease in weight is shown by more planktonic species suggests that the decrease could be due to dissolution. Consequently, morphological characteristics such as the thin, foraminiferal shells with large pores as described by Capotondi et al. (1999) in the Ecozone 4 (9–7.2 kyr) could not be a primary species-specific phenotypic variation.

4.2. Paleoecological reconstruction of the S1 interval based on micropaleontological and geochemical data

The distribution of modern planktonic foraminifera is principally linked to physical and chemical properties of the surface water masses where they live. The different environmental preferences of these organisms allow a reconstruction of past oceanographic conditions based on their spatial and temporal distribution (Thunell, 1978). The collection of time series samples has improved understanding of planktonic foraminiferal ecology, marking the importance of parameters such as, among others, the pycnocline and chlorophyll maximum depths, the thickness of the mixed layer, and stratification of the water column. All these parameters control food availability and the reproductive cycles of these organisms (Pujol and Vergnaud Grazzini, 1995).

Coccolithophores are directly dependent on environmental gradients in nutrients and sunlight (Brand, 1994). In the modern Mediterranean, species show seasonal variations in fluxes associated with oceanographic changes occurring between summer and winter months (Knappertsbusch, 1993; Ziveri et al., 2000; Malinverno et al., 2003).

In the following we will try to reconstruct the biogeochemical environment during the sapropel deposition by an integrated interpretation of micropaleontological and geochemical data obtained from box core SL9.

Changes in the composition of foraminiferal assemblage indicate the occurrence of at least three different ecological stages during S1 deposition (Principato et al., 2003; this work, Fig. 2). Here, we mainly focus on the fluctuations in accumulation rate of calcareous nannofossils and only shortly summarise the paleoecological interpretation of the foraminifera patterns since this is discussed by Principato et al. (2003).

The pre-sapropel/S1 lower interval (before 9.2 kyr BP; ~PF3/PF4a boundary) is characterised by an increase of *G. sacculifer* and *N. pachyderma* dextral with the presence of few *G. inflata* specimens and *T. truncatulinoides* as shown by both the relative abundance and the pfAR curves. According to Principato et al. (2003), the occurrence of both *G. inflata* and *T. truncatulinoides* confirms the presence of an isothermal water mass with deep convective mixing just before sapropel formation. The species *G. ruber* is exclusively represented by the *alba* variety and more compact morphotypes, such as *G. gomitulus*, are dominant. Violanti et al. (1991) documented the presence of these forms in warm-temperate sedimentary intervals, whereas they observed the absence during climatic optimum phases such as those occurring during the formation of sapropels S1 and S5. The weakly shifted *G. sacculifer* positive trend at the base of S1 indicates the occurrence of a shallow pycnocline, possibly linked to a strong runoff period, and, at the same time, the development of the Deep Chlorophyll Maximum (DCM), a high productivity layer in the lower part of the photic zone. According to Bianchi et al. (2006), processes responsible for an increase in sedimentation velocity of particulate organic matter can produce a redistribution of nutrients in the photic zone, supporting the occurrence of the DCM and the re-arrangement of the ecosystem structure.

The presence of a DCM during sapropel deposition was initially suggested by Castradori (1993) on the basis of increases in abundance of *F. profunda*, a typical lower photic zone species from low–middle latitude regions (Okada and Honjo, 1973). Successive studies demonstrated the basin-wide repetition of the pattern of this species (Negri and Giunta, 2001; Corselli et al., 2002; Principato et al., 2003; Thomson et al., 2004).

Differently from *F. profunda*, the surface water coccolith *E. huxleyi* shows a decreasing trend in abundance during the same interval. This species is very sensitive to an increase in nutrients and can produce huge surface–water blooms (Young, 1994; Winter et al., 1994; Nanninga and Tyrrell, 1996). In the oligotrophic Mediterranean basin, peaks in abundance of *E. huxleyi* are responsible for the seasonal coccolithophore production at winter wind-driven breakdown of stratification (Knappertsbusch, 1993; Ziveri et al., 2000). Nonetheless, in the modern eastern Mediterranean, fluxes of *F. profunda* parallel *E. huxleyi* production (Ziveri et al., 2000). A similar production of the two species is observed from more productive tropical and equatorial areas with *F. profunda* being often on average more common than *E. huxleyi* (Tanaka and Kawahata, 2001). In contrast, during sapropel deposition the anti-correlation of fluxes of these two species suggests an increased fertility in deep photic zone. The pattern of the paleoflux of *E. huxleyi* suggests low fertility of the surface waters. This interpretation is supported by the moderate paleofluxes of *Rhabdosphaera* spp. The group includes upper photic zone warm water species with a marked preferences for low nutrient concentration (Okada and Honjo, 1973; Roth and Coulbourn, 1982; Winter et al., 1994). In the waters of the modern Mediterranean, *Rhabdosphaera* species are commonly concentrated in the upper 5 m (Malinverno et al., 2003).

The highest coccolithophore diversity is found in stratified and oligotrophic waters. In highly eutrophic domains, few species dominate (e.g., Winter et al., 1994). A decrease in simple diversity occurs within S1 (Fig. 3b), and a similar pattern is obtained when the holococcoliths, represented by 8 taxa and that are likely dissolved within the sapropel (Crudeli et al., in press), are not considered in the calculation. Possible selective dissolution of other forms suggests, however, caution in the interpretation of the decrease in diversity.

High fertility conditions during the S1 time are also recorded by the increasing trend in relative abundance of *T. quinqueloba*, a foraminiferal species living in the photic zone (Bè and Tolderlund, 1971). The increase in abundance of this small and cold water species in the sapropel S1 deposited during warm climatic conditions suggests its strong link with periods of low water density, highly stratified water column in concurrence with high nutrients and terrestrial organic material input (Capotondi et al., 2004).

The trends in Ba/Al and C_{org} (%) could be explained by the increase in productivity in the lower photic zone recorded by *F. profunda* and a contemporaneous in-

crease in organic matter preservation due to the establishment of an anoxic environment at the bottom (Fig. 6b, c). C_{org} contents in the sapropel (Fig. 6c) are comparable to C_{org} values recorded in S1 (1–3.4%) from various areas of the eastern Mediterranean (Murat and Got, 2000).

The S1 medium interval (~7.5–9.2 kyr BP) is characterised by the maximum increase in relative abundance of *G. ruber* (*alba* and *rosea*) and *G. bulloides* with an abrupt decrease and temporary disappearance of *G. sacculifer*, *N. pachyderma* dextral and *G. inflata*. The maximum increase in accumulation rate of *G. ruber* occurs within the oxidized S1 interval.

In the present Mediterranean Sea, *G. ruber* proliferates during summer in nutrient-depleted warm surface water, and therefore its abundance in S1 could mark the real climatic optimum phase and maximum stratification conditions in the water column. In this interval, the morphotype *G. ruber* s.s. is dominant and its *rosea* variety, the warmest form of this species, occurs in significant amounts.

Foraminiferal diversity shows a clear decrease in this interval, suggesting critic conditions also in surface waters; at the same time, benthic foraminifera totally disappear because of the establishment of anoxia at the bottom. In the same interval, *G. bulloides* also increases both in relative abundance and accumulation rate. This species can live in near-surface waters during times of high productivity but often can occur within a subsurface chlorophyll maximum beneath the mixed layer and the thermocline as stratification increases (Pujol and Vergnaud Grazzini, 1995; Field, 2004).

Changes in the paleoecological conditions of the water column throughout this interval are traced by various coccolithophores species (e.g., *H. carteri* and small *Helicosphaera* spp.). *H. carteri* and *H. hyalina*, previously distinguished at variety level, have been shown to be separate species (Sáez et al., 2003). In the modern Mediterranean, *H. carteri* is relatively common, but the other species are rare (Cros, 2002). *H. carteri* is a eutrophic species (Ziveri et al., 2004) and proliferates between 40 and 70 m close to the chlorophyll maximum (Cros et al., 2000; Cros, 2002). Its increase in fluxes during S1 formation (Fig. 5) indicates nutrient availability at depth. The roughly opposite trend of *S. pulchra* (Fig. 5) is related to the different ecology of the species (Ziveri et al., 2004 and references therein). This species increases in oligotrophic stratified waters such as the tropical Atlantic Gyres. The ecology of species included in the *Helicosphaera* spp. group is less known. *H. hyalina* and/or *H. pavimentum* are rare to occasional in the equatorial tropical and subtropical zone of the Pacific and in the equatorial Atlantic (Okada and McIntyre, 1977; Steinmetz, 1991). The parallel increase in S1 of *Helicosphaera* spp. and *H. carteri* suggests ecological affinity. This may be expected since these are sister species (Sáez et al., 2003). Nonetheless, the fact that *Helicosphaera* spp. decrease and disappear upward suggests that these forms have a more restricted ecology. Their pattern suggests that the ecological conditions deteriorated after about 6.5 kyr BP.

In the upper part of this interval, the reoccurrence of the three species *G. sacculifer*, *N. pachyderma* dextral and *G. inflata* marks a significant change in the upper water column, as confirmed by the almost contemporaneous (at ~8 kyr BP) significant decrease in both the Ba/Al and C_{org} profiles (dotted interval in Figs. 6 and 7). At the same time, a small negative peak in sand content (Fig. 7), possibly related to a general decrease in biogenic production is also well recorded in core SL9. The brief decrease in Ba/Al and C_{org} is possibly related to the interruption in sapropel deposition recorded in other Mediterranean areas (Perissoratis and Piper, 1992; Rohling et al., 1997; De Rijk et al., 1999; Mercone et al., 2000). Both these geochemical proxies may be linked to primary production (Thomson et al., 1995, 1999; Van Santvoort et al., 1996), so that their decrease could record a temporary change in the planktonic and benthic ecosystem and, at the same time, in deep water circulation that even led to re-oxygenation in some areas (Adriatic and Aegean Seas). Therefore, it is possible that the geochemical change detected in core SL9 at ~8 kyr BP is linked to the short climatic deterioration that is suggested to be responsible for the S1 interruption (Mercone et al., 2000).

The S1 upper interval (about 5.5–7.5 kyr BP; near PF1a/PF2 boundary) is marked by an increasing trend in abundance of *G. sacculifer*, *N. pachyderma* dextral and *G. inflata* in both the curves. This foraminiferal assemblage suggests the reoccurrence of a shallow pycnocline, immediately followed by a well mixed water column that is consistent with the breaking of stratification. Foraminiferal diversity clearly increases in this interval, reaching the values of normal pelagic conditions. Benthic foraminifera reoc-

cur in detectable quantities, confirming the start of a re-oxygenation process at the bottom. In particular, the short and abrupt increase in foraminiferal simple diversity is approximately coincident with the significant decrease of cnAR and pfAR (Fig. 7) and exactly corresponds to the strong decrease in Ba/Al concentration in the sediment that marks the real top of the sapropel and the final breaking of water column stratification.

The major decrease in paleofluxes of *F. profunda*, corresponding with an increase of the total nannoflora after about 6.5 kyr BP, suggests a switch in productivity from the lower to the upper photic zone and a reestablishment of "normal" nutrient availability in the surface water.

U. sibogae is a species that is characteristic for the intermediate layer of the tropical–subtropical zone and prefers oligotrophic water (McIntyre and Be, 1967; Okada and McIntyre, 1979; Reid, 1980; Winter et al., 1994). Nonetheless, *Umbilicosphaera*, as other placolith-bearing coccolithophores, has a tendency toward eutrophic adaptation (Young, 1994 and references therein). The increase in accumulation rate of *Umbilicosphaera* spp. starting just before the S1 termination (about 7.5 kyr BP) is consistent with the nutrient redistribution in the surface water recorded by the general increase of *E. huxleyi* as well as with the permanence of the general oligotrophic condition of the Mediterranean surface water. This is also suggested by moderate but continuous fluxes in and outside S1 of *U. tenuis*, a typical oligotrophic form (Winter et al., 1994) occurring at 50–75 m water depth in nitrate depleted waters (Cortés et al., 2001). As discussed above, pronounced variations contemporarily characterise the foraminiferal assemblage. It is therefore probable that an early re-establishment of normal surface water ecological conditions occurred before the end of the sapropel deposition.

4.3. Sapropel formation and plankton productivity

Sapropel formation has been suggested to require both density stratification of the water column and increased primary productivity (Rohling, 1994; Strohle and Krom, 1997). Surface water productivity can be estimated from the benthic flux of organic carbon by applying various empirical flux equations (e.g., Suess, 1980). Benthic foraminiferal accumulation rates (bfAR; Fig. 7) also can be used as a proxy of paleocarbon fluxes (de Stigter et al., 1996). Here, we tentatively reconstruct changes in surface productivity by the integration of bfAR, pfAR and cnAR trends. Estimation of paleocarbon fluxes can be complicated by the fact that most of the organic carbon arriving to the seafloor is relatively rapidly remineralized or recycled as benthic biomass, and so only a minor proportion is preserved in the sediment. The enhanced C_{org} burial rate during sapropel S1 leads to enhanced preservation of organic carbon in the bottom sediments, protecting it from remineralization. At the same time, both pelagic and benthic bacteria decomposing particulate organic material produced by all the surface water living groups consume oxygen and favour anoxia establishment at the bottom (Bianchi et al., 2006). The bfAR decreases in most of S1 of the SL9 core and shows 0 values in the lower–middle part of the sapropel (Fig. 7). The benthic forms usually require oxygen to survive, so they were strongly affected by the extreme oxygen deficiency at the seafloor during S1 deposition rather than by the paleocarbon flux.

In the lower part of S1, calcareous nannofossil and foraminiferal total accumulation rates are moderate and increase in the upper part of sapropel. As previously discussed, planktonic assemblages are likely not heavily affected by dissolution, and the significant changes in fluxes and species composition of the assemblages (Figs. 2, 5, and 7) record important paleoecological variations that occurred during the deposition of the sapropel.

The formation of sapropel S5 (125 kyr) occurred during a general warming phase (Marine Isotopic Stage 5e), a climatic stage similar to that of the deposition of sapropel S1 (MIS1) (Emeis et al., 2003). The main difference between these two sapropels is the preservation in S5 of diatoms and other siliceous microfossils in finely laminated intervals alternated with more terrigenous levels that record annual flux cycles (Kemp et al., 1999; Corselli et al., 2002). No siliceous microfossils are recorded in S1. There is, however, a similarity between calcareous nannofossil and planktonic foraminiferal assemblages in sapropels S5 and S1 (Corselli et al., 2002; this work, relative abundance data, respectively) as here summarised. *F. profunda* and small *Helicosphaera* spp. increase in abundance within the organic-rich interval, a peak in relative abundance of *Umbilicosphaera* spp. occurs just after the top of sapropel S5 in correspondence with a major decrease of diatoms (Corselli et al., 2002), *G. ruber alba* and *rosea* show a positive trend in relative abundance in the lowest part of both sapropels, and *G. inflata* disappears at the beginning of anoxia in both sapropels. The similar patterns of pelagic organisms documented in two temporally distinct sapropels suggest the occurrence of similar paleoecological conditions in the water

column. So, despite the absence of diatoms in S1 sediments, it may be possible that these were productive during the deposition of sapropel S1. In particular, in S1 sediments some organic compounds related to silica-shelled organisms such as diatoms were detected (SAP Project Final Summary, 2001) and would support the previous hypothesis. During sapropel S5 deposition, the paleoceanographic conditions favoured proliferation either of diatoms and *F. profunda* in a DCM (Kemp et al., 1999; Corselli et al., 2002, respectively) as also recorded in S1 from core SL9 by the increase in paleofluxes of *F profunda*.

Significant changes in the composition of microplanktonic assemblages imply that the S1 deposition was a complex event, characterised by distinct phases and probably marked by short-term climatic changes (Principato et al., 2003; Giunta et al., 2003; this work, Figs. 2 and 5).

On-going studies coupling geochemical and paleobiological approaches, together with a comparison with independent proxies, will better constrain the sources of organic matter in the sapropels and the major mechanism leading to their formation. In particular, it is a central theme to separate preservation from bio-productivity, taking into account that proxies for productivity suffer from modifications such as dissolution, aerobic decay, and migration (e.g., Versteegh and Zonneveld, 2002).

5. Conclusions

Based on relative abundance and accumulation rates of calcareous nannofossils, planktonic foraminifera and pteropods, we reconstructed the paleoecological–paleoenvironmental variations that occurred in the upper water column during the deposition of the Holocene sapropel S1 in the eastern Mediterranean. In particular, the quantification of the assemblages in terms of accumulation rates provided an estimation of absolute variations in primary and secondary productivity during sapropel S1 formation. The study of foraminiferal weight variations in and outside the sapropel and the evaluation of pteropod occurrence allowed a qualitative estimation of carbonate dissolution in sapropel S1 sediments. At the same time, the integration of these results with changes in accumulation rate of the major calcareous nannofossil species allowed an estimation of the possible intensity of corrosion processes on calcareous biogenic material. We observed that the three analysed foraminiferal species show a clear decrease in weight into the sapropel. The same interval is also characterised by the absence of selected holococcoliths, other delicate forms of coccoliths (*G. flabellatus* and *A. robusta*) and pteropods, likely because of moderate dissolution processes. Also the decrease in accumulation rate of the most abundant calcareous nannofossil species *E. huxleyi* in S1 may be weakly biased by changes in preservation.

After evaluation of possible dissolution effects in the planktonic assemblages, environmental variations during S1 deposition were reconstructed as follows. The decrease in accumulation rate of the total UPZ-MPZ nannoflora within most of the S1 interval suggests moderate productivity in surface waters. By contrast, the significant increase in paleofluxes of *F. profunda* suggests that the lower photic zone was nutrient-rich. These changes in paleoecological conditions occurred before the sapropel started to form at the seafloor. Trends in Ba/Al curves within the sapropel are in accordance with the increase in productivity in the lower photic zone recorded by *F. profunda*.

The beginning of S1 deposition is characterised by the development of a shallow pycnocline recorded by *G. sacculifer* probably related to a runoff phase due to the intensification of the African monsoon. The increased paleofluxes of *Helicosphaera* species are likely related to the nutrification conditions in the middle part of the photic zone that occurred from the beginning of S1 formation until about 6.5 kyr BP, as also suggested by the increase in accumulation rate of *G. bulloides*. The increase in relative abundance of *G. ruber alba* and *rosea* in the lower part of sapropel marks the climatic optimum phase and the maximum stratification in the upper water column, whereas the contemporaneous disappearance of benthic foraminifera record anoxia at the sea floor.

A transition phase ("interruption") is recorded by a negative peak in Ba/Al and C_{org} within the S1 layer at ~8 kyr BP. During this short interval, the general biogenic production most likely decreased, as indicated by the contemporaneous negative shift in the sand content.

Just after the mid-sapropel transition phase, the reoccurrence of the three foraminiferal species *G. sacculifer*, *N. pachyderma* dextral and *G. inflata* marks a significant change in the upper water column. In particular the reappearance of the last species records the development of frontal systems in the surface/subsurface water, leading to the breaking of stratification before the end of sapropel deposition. At the same time, the reoccurrence of benthic foraminifera in the oxidized S1 underlines that the bottom conditions also started to change gradually during the last stages of sapropel deposition.

Acknowledgements

This study was supported by the EU Marine Science and Technology Framework V Project "Sapropels And Paleoceanography" (MAS3-CT97-0137) and by the European CODENET (Coccolithophorid evolutionary biodiversity and ecology network) project (FRMX-ET97-0113). Silvia Spezzaferri and Mario Cachao are acknowledged for their helpful and constructive revision.

References

Bairbakhish, A.N., Bollmann, J., Sprengel, C., Thierstein, H.R., 1999. A technique for disintegration of aggregates and coccospheres in sediment trap samples. Mar. Micropaleontol. 37, 218–223.

Bè, A.W.H., Tolderlund, D.S., 1971. Distribution and ecology of living planktonic foraminifera in surface waters of the Atlantic and Indian oceans. In: Funnel, B.M., Riedel, W.R. (Eds.), The Micropaleontology of the Oceans, pp. 105–149.

Berner, R.A., Honjo, S., 1981. Pelagic sedimentation of aragonite: its geochemical significance. Science 211, 940–942.

Bianchi, D., Zavatarelli, M., Pinardi, N., Capozzi, R., Capotondi, L., Corselli, C., Masina, S., 2006. Simulations of ecosystem response during the sapropel S1 deposition event. Palaeogeogr. Palaeoclimatol. Palaeoecol. 235, 265–287 (this volume).

Brand, L.E., 1994. Physiological ecology of marine phytoplankton. In: Winter, A., Siesser, W. (Eds.), Coccolithophores. Cambridge University Press, Cambridge, pp. 39–49.

Broecker, W.S., Clark, E., 2001. Glacial to Holocene redistribution of carbonate ion in the deep sea. Science 294, 2152–2155.

Broecker, W.S., Clark, E., 2002. Carbonate ion concentration in glacial-age deep waters of the Caribbean Sea. Geochem. Geophys. Geosyst. 3 (3) (electronic journal of the Earth Sciences, published by AGU and the Geochemical Society).

Broecker, W.S., Linch-Stieglitz, J., Clark, E., Hajdas, I., Bonani, G., 2001. What caused the atmosphere's CO_2 content to rise during the last 8000 years? Geochem. Geophys. Geosyst. 2 (electronic journal of the Earth Sciences, published by AGU and the Geochemical Society).

Calvert, S.E., 1983. Geochemistry of Pleistocene sapropels and associated sediments from the eastern Mediterranean. Oceanol. Acta 6, 225–267.

Calvert, S.E., Fontugne, M.R., 2001. On the late Pleistocene–Holocene sapropel record of climatic and oceanographic variability in the eastern Mediterranean. Paleoceanography 16 (1), 78–94.

Capotondi, L., Borsetti, A.M., Morigi, C., 1999. Foraminiferal ecozones, a high resolution proxy for the late Quaternary biochronology in the central Mediterranean Sea. Mar. Geol. 153, 253–274.

Capotondi, L., Soroldoni, E., Principato, M.S., Corselli, C., 2004. Statistical approach for late Quaternary paleoceanographic reconstructions: importance of size fraction. Proceedings of the First Italian Meeting of Environmental Micropaleontology, The Grzybowski Foundation Special Publication, vol. 9.

Castradori, D., 1992. I nannofossili calcarei come strumento per lo studio biostratigrafico e paleoceanografico del Quaternario nel Mediterraneo Orientale. PhD thesis, University of Milan, Italy.

Castradori, D., 1993. Calcareous nannofossils and the origin of eastern Mediterranean sapropels. Paleoceanography 8 (4), 459–471.

Cita, M.B., Vergnaud-Grazzini, C., Robert, C., Chamley, H., Ciaranfi, N., D'Onofrio, S., 1977. Paleoclimatic record of a long deep sea core from the eastern Mediterranean. Quat. Res. 8, 205–235.

Corselli, C., Principato, M.S., Maffioli, P., Crudeli, D., 2002. Changes in planktonic assemblages during sapropel S5 deposition: evidence from Urania Basin area, eastern Mediterranean. Paleoceanography 17 (3), 1–30.

Cortés, M.Y., Bollmann, J., Thierstein, H.R., 2001. Coccolithophore ecology at the HOT station ALOHA, Hawaii. Deep-Sea Res. II 48, 1957–1981.

Cramp, A., O'Sullivan, G., 1999. Neogene sapropels in the Mediterranean: a review. Mar. Geol. 153, 11–28.

Cros, M.L., 2002. Planktonic Coccolithophores of the NW Mediterranean. Publicacions de la Universitat de Barcelona, Barcelona.

Cros, L., Kleijne, A., Zeltner, A., Billard, C., Young, J.R., 2000. New examples of holococcolith-heterococcolith combination coccospheres and their implications for coccolithophorid biology. Mar. Micropaleontol. 39, 1–34.

Crudeli, D., Young, J.R., 2003. SEM-LM study of holococcoliths preserved in eastern Mediterranean sediments (Holocene/late Pleistocene). J. Nannoplankton Res. 25 (1), 39–50.

Crudeli, D., Young, J.R., Erba, E., de Lange, G.J., Henriksen, K., Kinkel, H., Slomp, C.P., Ziveri, P., 2004. Abnormal carbonate diagenesis in Holocene-late Pleistocene sapropel-associated sediments from eastern Mediterranean; evidence from *Emiliania huxleyi* coccolith morphology. In: Villa, G., Lees, J.A., Bown, P.R. (Eds.), Calcareous Nannofossil Palaeoecology and Palaeoceanographic Reconstructions, Marine Micropaleontol., Special Issue, vol. 52/1–4, pp. 217–240.

Crudeli, D., Young, J.R., Erba, E., Geisen, M., Ziveri, P., de Lange, G.J., Slomp, C.P., in press. Fossil record of holococcoliths and selected hetero-holococcolith associations from the Mediterranean (Holocene–late Pleistocene): evaluation of carbonate diagenesis and palaeoecological–palaeoceanographic implications. Palaeogeogr. Palaeoclimatol. Palaeoecol.

De Lange, G.J., ten Haven, H.L., 1983. Recent sapropel formation in the eastern Mediterranean. Nature 305, 797–798.

De Lange, G.J., Middelburg, J.J., Pruysers, P.A., 1989. Middle and Late Quaternary depositional sequences and cycles in the eastern Mediterranean. Sedimentology 36, 151–158.

De Lange, G.J., Van Santvoort, P.J.M., Langereis, C., Thomson, J., Corselli, C., Michard, A., Rossignol-Strick, M., Paterne, M., Anastasakis, G., 1999. Palaeo-environmental variations in eastern Mediterranean sediments; a multidisciplinary approach in a prehistoric setting. Prog. Oceanogr. 44, 369–386.

De Rijk, S., Hayes, A., Rohling, E.J., 1999. Eastern Mediterranean sapropel S1 interruption: an expression of the onset of climatic deterioration around 7 ka BP. Mar. Geol. 153, 337–343.

de Stigter, H.C., Jorissen, F.J., van der Zwaan, G.J., 1996. Evidence for the control of organic carbon flux on the bathymetric zonation of benthic foraminifera. In: de Stigter, H.C., (Ed.), Geologica Ultraiectina vol. 144, pp. 121–142.

Emeis, K.-C., Shulz, H., Struck, U., Rossignol-Strick, M., Erlenkeusen, H., Howell, M.W., Kroon, D., Mackensen, A., Ishizuka, S., Oba, T., Sakamoto, T., Koizumi, I., 2003. Eastern Mediterranean surface water temperatures and $\delta^{18}O$ composition during deposition of sapropels in the late Quaternary. Paleoceanography 18 (1), 1–18.

Field, D.B., 2004. Variability in vertical distributions of planktonic foraminifera in the California Current: relationships to vertical ocean structure. Paleoceanography 19, 1–22.

Fontugne, M.R., Calvert, S.E., 1992. Late Pleistocene variability of the carbon isotopic composition of organic matter in the eastern Mediterranean: monitor of changes in carbon sources and atmospheric CO_2 levels. Paleoceanography, 16, 1, 78–94.

Giraudeau, J., Pierre, C., Herve, L., 2001. A late Quaternary, high-resolution record of planktonic foraminiferal species distribution in the southern Benguela region: Site 1087. In: Wefer, G., Berger, W.H., Richter, C., (Ed.), Proc. ODP, Scient. Res., vol. 175, pp. 1–26.

Giunta, S., Negri, A., Morigi, C., Capotondi, L., Combourieu-Nebout, N., Emeis, K.C., Sangiorgi, F., Vigliotti, L., 2003. Coccolithophorid ecostratigraphy and multi-proxy paleoceanographic reconstruction in the Southern Adriatic Sea during the last deglacial time (Core AD91-17). Palaeogeogr. Palaeoclimatol. Palaeoecol. 190, 39–59.

Hemleben, Ch., Spindler, M., Anderson, O.R., 1989. Modern Planktonic Foraminifera. Springer-Verlag Eds. 363 pp.

Herman, Y., 1981. Paleoclimatic and paleohydrologic record of Mediterranean deep-sea cores based on pteropods, planktonic and benthonic foraminifera. Rev. Espan. de Micropaleontol., XIII 2, 171–200.

Howell, M.W., Thunell, R.C., 1992. Organic carbon accumulation in Bannock Basin: evaluating the role of productivity in the formation of eastern Mediterranean sapropels. Mar. Geol. 103, 461–471.

Ivanova, E.M., 1999. Late Quaternary monsoon history and paleoproductivity of the western Arabian Sea. Thesis Amsterdam, pp. 1–172.

Jordan, R.W., Kleijne, A., 1994. A classification system for living coccolithophores. In: Winter, A., Siesser, W.G. (Eds.), Coccolithophores. Cambridge University Press, Cambridge, pp. 83–105.

Jorissen, F.J., Asioli, A., Borsetti, A.M., Capotondi, L., de Visser, J.P., Hilgen, F.J., Rohling, E.J., van der Borg, K., Vergnaud-Grazzini, C., Zachariasse, W.J., 1993. Late Quaternary central Mediterranean biochronology. Mar. Micropaleontol. 21, 169–189.

Kemp, A.E.S., Pearce, R.B., Pike, J., Koizumi, I., Rance, S.J., 1999. The role of mat-forming diatoms in the formation of Mediterranean sapropels. Nature 398. , 57–61.

Kleijne, A., 1992. Extant Rhabdosphaeraceae (coccolithophorids, class Prymnesiophyceae) from the Indian Ocean, Red Sea, Mediterranean Sea and North Atlantic Ocean. Scr. Geol. 100, 1–63.

Knappertsbusch, M., 1993. Geographic distribution of living and Holocene coccolithophores in the Mediterranean Sea. Mar. Micropaleontol. 21, 219–247.

Malinverno, E., Ziveri, P., Corselli, C., 2003. Coccolithophorid distribution in the Ionian Sea and its relationship to eastern Mediterranean circulation during late fall-early winter 1997. J. Geophys. Res. 108 (C9), 8115.

Matsuoka, H., Okada, H., 1989. Quantitative analysis of Quaternary nannoplankton in the subtropical northwestern Pacific Ocean. Mar. Micropaleontol. 14, 97–118.

McIntyre, A., Be, A.W.H., 1967. Modern coccolithophoridae of the Atlantic Ocean: I. Placoliths and cyrtoliths. Deep-Sea Res. 14, 561–597.

Mercone, D., Thomson, J., Croudace, I.W., Siani, G., Paterne, M., Troelstra, S., 2000. Duration of S1, the most recent sapropel in the eastern Mediterranean Sea, as indicated by accelarator mass spectrometry radiocarbon and geochemical evidence. Paleoceanography 15, 336–347.

Meyers, P.A., Doose, H., 1999. Sources, preservation and thermal maturity of organic matter in Pliocene–Pleistocene organic-carbon-rich-sediments of the western Mediterranean Sea. In: Zahn, R., Comas, M.C., Klaus, A., (Ed.), Proceed. O.D.P., Scient. Res., vol. 161, pp. 383–390.

Murat, A., Got, H., 2000. Organic carbon variations of the eastern Mediterranean Holocene sapropel: a key for understanding formation processes. Palaeogeogr. Palaeoclimatol. Palaeoecol. 158, 241–257.

Nanninga, H.J., Tyrrell, T., 1996. The importance of light for the formation of algal blooms by *Emiliania huxleyi*. Mar. Ecol., Prog. Ser. 136, 195–203.

Negri, A., Giunta, S., 2001. Calcareous nannofossil paleoecology in the sapropel S1 of the eastern Ionian sea: paleoceanographic implications. Palaeogeogr. Palaeoclimatol. Palaeoecol. 169, 101–112.

Negri, A., Giunta, S., Hilgen, F., Krjigsman, W., Vai, G.B., 1999. Calcareous nannofossil biostratigraphy of the M. del Casino section (northern Apennines, Italy) and paleoceanographic conditions at times of Late Miocene sapropel formation. Mar. Micropaleontol. 36 (1), 13–30.

Negri, A., Morigi, C., Giunta, S., 2003. Are productivity and stratification important to sapropel deposition? Microfossil evidence from late Pliocene insolation cycle 180 at Vrica. Calabria. Palaeogeogr. Palaeoclimatol. Palaeoecol. 190, 243–255.

Okada, H., Honjo, S., 1973. The distribution of oceanic coccolithophores in the Pacific. Deep-Sea Res. 20, 355–374.

Okada, H., McIntyre, A., 1977. Modern coccolithophores of the Pacific and North Atlantic Oceans. Micropaleontology 23 (1), 1–56 (pls. 1–13, (483)).

Okada, H., McIntyre, A., 1979. Seasonal distribution of modern coccolithophores in the western North Atlantic Ocean. Mar. Biol. 54, 319–328.

Passier, H.F., Dekkers, M.J., 2002. Iron oxide formation in the active oxidation front above sapropel S1 in the eastern Mediterranean Sea as derived from low-temperature magnetism. Geophys. J. Int. 150. , 230–240.

Perissoratis, C., Piper, D.J.W., 1992. Age, regional variation and shallowest occurrence of S1 sapropel in the northern Aegean Sea. Geo-Mar. Lett. 12, 49–53.

Principato, M.S., 2003. Late Pleistocene–Holocene planktonic foraminifera from the eastern Mediterranean Sea: based on a paleoclimatic interpretation a high resolution quantitative study. Riv. Ital. Paleontol. Stratigr. 109 (1), 111–124.

Principato, M.S., Giunta, S., Corselli, C., Negri, A., 2003. Late Pleistocene/Holocene planktonic assemblages in three box-cores from the Mediterranean Ridge area (W-SW of Crete): paleoecological and paleoceanographic reconstruction of sapropel S-1 interval. Palaeogeogr. Palaeoclimatol. Palaeoecol. (Special Issue) 190, 61–77.

Pujol, C., Vergnaud Grazzini, C., 1995. Distribution patterns of live planktic foraminifers as related to regional hydrography and productive systems of the Mediterranean Sea. Mar. Micropaleontol. 25, 187–217.

Reid, F.M.H., 1980. Coccolithophorids of the North Pacific Central Gyre with notes on their vertical and seasonal distribution. Micropaleontology 26 (2), 151–176.

Rohling, E.J., 1994. Review and new aspects concerning the formation of eastern Mediterranean sapropels. Mar. Geol. 122. 1–28.

Rohling, E.J., Jorissen, F.J., De Stigter, H.C., 1997. 200 year interruption of Holocene sapropel formation in the Adriatic Sea. J. Micropaleontol. 16 (2), 97–108.

Rossignol-Strick, M., 1985. Mediterranean Quaternary sapropels, an immediate response of the African Monsoon to variation of insolation. Palaeogeogr. Palaeoclimatol. Palaeoecol. 49, 237–263.

Roth, P.H., Berger, W.H., 1975. Distribution and dissolution of coccoliths in the South and central Pacific. Cushman Found. Foraminiferal Res. 13, 87–113.

Roth, P.H., Coulbourn, W.T., 1982. Floral and dissolution patterns of coccoliths in surface sediments of the North pacific. Mar. Micropaleontol. 7, 1–52.

Rutten, A., de Lange, G.J., Ziveri, P., Thomson, J., van Santvoort, P.J.M., Colley, S., Corselli, C., 2000. Recent terrestrial and carbonate fluxes in the pelagic eastern Mediterranean; a comparison between sediment trap and surface sediment. Palaeogeogr. Palaeoclimatol. Palaeoecol. 158, 197–213.

Sáez, A.G., Probert, I., Geisen, M., Quinn, P., Young, J.R., Medlin, L.K., 2003. Pseudo-cryptic speciation in coccolithophores. Proc. Natl. Acad. Sci. 100 (12), 7163–7168.

Sancetta, C., 1994. Mediterranean sapropels: seasonal stratification yields high production and carbon flux. Paleoceanography 9, 195–196.

Sapropels And Paleoceanography (SAP Project) Final Summary, 2001. MUST III Program of European Union (EU).

Sbaffi, L., Wezel, F.C., Kallel, N., Paterne, M., Cacho, I., Ziveri, P., Shackleton, 2001. Response of the pelagic environment to palaeoclimatic changes in the central Mediterranean Sea during the Late Quaternary. Mar. Geol. 178, 39–62.

Schmiedl, G., Mitschele, A., Beck, S., Emeis, K.-C., Hemleben, C., Schulz, H., Sperling, M., Weldeab, S., 2003. Benthic foraminiferal record of ecosystem variability in the eastern Mediterranean Sea during times of sapropel S5 and S6 deposition. Palaeogeogr. Palaeoclimatol. Palaeoecol. 190, 139–164.

Steinmetz, J.C., 1991. Calcareous nannoplankton biocoenosis: sediment trap studies in the Equatorial Atlantic, Central Pacific, and Panama Basin. In: Honjo, S., (Ed.), Ocean Biocoenosis Series, vol. 1. Woods Hole Oceanographic Institution, pp. 1–85.

Steinmetz, J.C., 1994. Sedimentation of coccolithophores. In: Winter, A., Siesser, W.G. (Eds.), Coccolithophores. Cambridge University Press, Cambridge, pp. 179–197.

Strohle, K., Krom, M.D., 1997. Evidence for the evolution of an oxygen minimum layer at the beginning of S-1 sapropel deposition in the eastern Mediterranean. Mar. Geol. 140, 231–236.

Suess, E., 1980. Particulate organic carbon flux in the ocean-surface productivity and oxygen utilization. Nature 280, 260–263.

Tanaka, Y., Kawahata, H., 2001. Seasonal occurrence of coccoliths in sediment taps from West Caroline Basin, equatorial West Pacific Ocean. Mar. Micropaleontol. 43, 273–284.

Ten Haven, H.L., De Leeuw, J.W., Schenk, P.A., Klaver, G.T., 1987. Geochemistry of Mediterranean sediments. Bromine/organic carbon and uranium/organic carbon ratios as indicators for different sources of input and post-depositional oxidation, respectively. Org. Geochem. 13, 255–261.

Thierstein, H.R., 1980. Selective dissolution of Late Cretaceous and earliest Tertiary calcareous nannofossils: experimental evidence. Cretac. Res. 2, 165–176.

Thomson, J., Higgs, N.C., Wilson, T.R.S., Croudace, I.W., De Lange, G.J., Van Santvoort, P.J.M., 1995. Redistribution and geochemical behaviour of redox-sensitive elements around S1, the most recent eastern Mediterranean sapropel. Geochim. Cosmochim. Acta 59, 3487–3501.

Thomson, J., Mercone, D., De Lange, J.G., Van Santvoort, P.J.M., 1999. Review of recent advances in the interpretation of eastern Mediterranean sapropel S1 from geochemical evidence. Mar. Geol. 153, 77–89.

Thomson, J., Crudeli, D., de Lange, G.J., Slomp, C.P., Erba, E., Corselli, C., Calvert, S.E., 2004. *Florisphaera profunda* and the origin and diagenesis of carbonate phases in eastern Mediterranean sapropel units. Paleoceanography 19, 1–19.

Thunell, R.C., 1978. Distribution of recent planktonic foraminifera in surface sediments of the Mediterranean Sea. Mar. Micropaleontol. 3, 147–173.

Van Santvoort, P.J.M., De Lange, G.J., Thomson, J., Cussen, H., Wilson, T.R.S., Krom, M.D., Strohle, K., 1996. Active post-depositional oxidation of the most recent sapropel (S1) in sediments of the eastern Mediterranean Sea. Geochim. Cosmochim. Acta 60, 4007–4024.

Versteegh, G.J.M., Zonneveld, K.A.F., 2002. Use of selective degradation to separate preservation from productivity. Geology 30 (7), 615–618.

Violanti, D., Grecchi, G., Castradori, D., 1991. Paleoenvironmental interpretation of core Ban 88-11GC (eastern Mediterranean, Pleistocene–Holocene-) on the grounds of Foraminifera, Thecosomata and calcareous nannofossils. Il Quaternario 4 (1a), 13–39.

Winter, A., Jordan, R.W., Roth, P.H., 1994. Biogeography of living coccolithophores in ocean water. In: Winter, A., Siesser, W.G. (Eds.), Coccolithophores. Cambridge University Press, Cambridge, pp. 171–177.

Young, J.R., 1994. Function of coccoliths. In: Winter, A., Siesser, W.G. (Eds.), Coccolithophores. Cambridge University Press, Cambridge, pp. 63–82.

Ziveri, P., Young, J.R., van Hinte, J.E., 1999. Coccolithophore export production and accumulation rates. On Determination of Sediment Accumulation Rates, GeoResearch Forum, vol. 5. Trans Tech Publications LTD, Switzerland, pp. 41–56.

Ziveri, P., Rutten, A., De Lange, G.J., Thomson, J., Corselli, C., 2000. Present-day coccolith fluxes recorded in central eastern Mediterranean sediment traps and surface sediments. Palaeogeogr. Palaeoclimatol. Palaeoecol. 158, 175–195.

Ziveri, P., Malinverno, E., Kinkel, H., Stoll, H., Principato, S., Corselli, C., Ganssen, G., 2001. A key study on a eastern Mediterranean core: testing paleoceanographic proxies. European Geophysical Society (EGS) XXVI General Assembly, Nice, France, March 2001.

Ziveri, P., Baumann, K.-H., Böckel, B., Bollmann, J., Young, J.R., 2004. Biogeography of selected Holocene coccoliths in the Atlantic Ocean. In: Thierstein, H.R., Young, J.R. (Eds.), Coccolithophores. From Molecular Processes to Global Impact, pp. 403–428.